Microbes and Infection 18 (2016) 565–571
www.elsevier.com/locate/micinf

Short communication

# Lipid droplets affect elimination of *Porphyromonas gingivalis* in HepG2 cells by altering the autophagy-lysosome system

Yumi Zaitsu [a], Mayumi Iwatake [a], Keiko Sato [b], Takayuki Tsukuba [a,*]

[a] *Division of Dental Pharmacology, Nagasaki University Graduate School of Biomedical Sciences, Sakamoto 1-7-1, Nagasaki, Nagasaki, 852-8588, Japan*
[b] *Division of Microbiology and Oral Infection, Nagasaki University Graduate School of Biomedical Sciences, Sakamoto 1-7-1, Nagasaki, Nagasaki, 852-8588, Japan*

Received 23 December 2015; accepted 17 May 2016
Available online 27 May 2016

**Abstract**

Recent studies have shown that infection with *Porphyromonas gingivalis*, a major periodontal pathogen, hastens the progression of non-alcoholic fatty liver disease (NAFLD). However, the intracellular fate of *P. gingivalis* in hepatocytes remains unknown. Here, using oleic-acid-induced HepG2 cells as an in vitro model for NAFLD, we found that lipid droplets increased the existence of *P. gingivalis* in the cells at an early phase of infection. Confocal microscopic analysis revealed that lipid droplets affected the formation of autolysosomes in infected cells. Thus, lipid droplets affect the elimination of *P. gingivalis* in HepG2 cells by altering the autophagy-lysosome system.


*Keywords:* *Porphyromonas gingivalis*; Non-alcoholic fatty liver disease; Autophagy; Lysosome; HepG2 cells

## 1. Introduction

*Porphyromonas gingivalis* is a gram-negative anaerobic bacterium that is involved in the etiology of progressive periodontal disease. Accumulating evidence has indicated that invasion of *P. gingivalis* from the oral cavity into the blood circulation causes several systemic diseases, such as cardiovascular diseases, diabetes mellitus, preterm low birth weight, and rheumatoid arthritis [1]. Recently, infection with *P. gingivalis* was reported to accelerate the development and progression of non-alcoholic fatty liver disease (NAFLD) [6,23]. In fact, the detected frequency of *P. gingivalis* in NAFLD patients was significantly higher than in non-diseased subjects [23]. Moreover, studies with mouse models revealed that infection with *P. gingivalis* promotes the pathological progression of NAFLD [6,23]. Since hepatic steatosis in NAFLD patients is characterized by intracellular accumulation of lipid droplets in hepatocytes, it is particularly important to determine the relationship between intracellular lipid droplets and pathogens. Some intracellular pathogens use lipid droplets either for nutritional purposes or as part of an anti-immunity strategy [14]. For example, *Mycobacterium* and *Chlamydia* species are parasitic on lipid droplets in macrophages, which they use as a nutrient source and to build up their own lipid inclusions [18]. However, the interaction between lipid droplets and *P. gingivalis* in hepatocytes remains unknown.

Several lines of evidence have shown that the intracellular fate of *P. gingivalis* is likely to be cell-type specific [7,19]. In endothelial cells, the internalized *P. gingivalis* is partially transported to lysosomes and otherwise to autophagosomes [3,4,22]. However, in gingival epithelial cells, a large number of internalized *P. gingivalis* are sorted into recycling endosomes and subsequently released into the extracellular space, although some of the intracellular bacteria were trafficked to lysosomes and autophagosomes [9,15,16,20]. However, the intracellular fate of *P. gingivalis* in hepatocytes remains to be elucidated. In this study, we have conducted such an investigation and further examined the host–pathogen interaction of

* Corresponding author. Tel.: +81 95 819 7652; fax: +81 95 819 7655.
*E-mail address:* tsuta@nagasaki-u.ac.jp (T. Tsukuba).

http://dx.doi.org/10.1016/j.micinf.2016.05.004
1286-4579/

*P. gingivalis* vs. lipid droplets (as hepatic steatosis) in hepatocytes. Therefore, we used the oleic-acid (OA)-induced hepatic steatosis of HepG2 cells as an in vitro model for NAFLD.

## 2. Materials and methods

### 2.1. Reagents

Polyclonal antibodies (Abs) were purchased as follows: anti-GAPDH (Cat. No. 5174S, D16H11, rabbit mAb, 1:1000) and anti-microtubule-associated protein 1 light chain 3 (LC3) (Cat. No. 12741, D3U4C rabbit mAb, 1:1000) were purchased from Cell Signaling Technology (Danvers, MA, USA); anti-lysosome-associated membrane protein 2 (LAMP2) was procured from Santa Cruz Biotechnology (Dallas, TX, USA; Cat. No. sc-18822, YL1/2, mouse monoclonal Ab). All other reagents including oleic acid (OA), bafilomycin $A_1$, phenylmethylsulfonyl fluoride and the protease inhibitor cocktail, were obtained from Sigma-Aldrich (St. Louis, MO, USA).

### 2.2. Bacterial strains and culture conditions

*P. gingivalis* ATCC 33277 was grown anaerobically (10% $CO_2$, 10% $H_2$, 80% $N_2$) in enriched brain heart infusion medium and on enriched trypticase soy agar as described previously [12]. The multiplicity of infection (MOI) was computed with reference to an optical density curve at 600 nm for the known colony-forming units. All the experiments were performed at an MOI of $10^2$.

### 2.3. Cell culture

HepG2 cells (RCB1886) were provided by the RIKEN BRC through the National Bio-Resource Project of MEXT, Japan. The HepG2 cells were cultured in Dulbecco's modified essential medium (D-MEM), containing 10% fetal bovine serum with 100 U/ml penicillin and 100 μg/ml streptomycin, under an atmosphere of 5% $CO_2$ at 37 °C with 95% humidity. For the induction of hepatic steatosis by OA, HepG2 cells were initially washed twice with phosphate-buffered saline (PBS) and subsequently added to medium containing 0–2.0 mM of an OA–bovine serum albumin (OA–BSA) complex (molar ratio 4:1). The cells were further incubated for 24 h to form lipid droplets. The medium with only BSA was selected as the control. Oil red O (ORO) staining was performed according to the method of Cui et al. [2] with some modifications.

### 2.4. Persistence assay

Prior to infection, HepG2 cells were washed with PBS and then suspended in kanamycin and fetal bovine serum-free D-MEM. The cells ($1 \times 10^5$ cells per well in 6-well tissue culture dishes) were infected with *P. gingivalis* for 20 min at an MOI of $10^2$. The infected cells were then washed and incubated in kanamycin-containing D-MEM for the indicated times. Before harvesting, gentamicin (300 μg/ml) and metronidazole (400 μg/ml) were added to the medium for 30 min to kill extracellular bacterial cells. The infected HepG2 cells were washed four times with PBS and then lysed in sterilized water by aspiration with 10 strokes using a syringe. The lysate was sequentially diluted and plated on anaerobic blood plate agar. The colonies on the plates were counted after anaerobic incubation at 37 °C for 7 days.

### 2.5. Immunofluorescence

Cells were fixed with 4% paraformaldehyde at 4 °C for 30 min, permeabilized with 0.01% digitonin for 10 min, and then blocked with 1% normal goat serum, followed by incubation with primary antibodies diluted with 1% normal goat serum. Incubation was carried out overnight at 4 °C. After three washes in PBS, primary antibodies were revealed with Alexa Fluor 488- or 555-conjugated anti-mouse or anti-rabbit antibodies (Cell Signaling Technology). To label bacterial and cellular DNAs, cells were stained using 4′,6-diamidino-2-phenylindole, dihydrochloride (DAPI; Sigma-Aldrich). Microscopic fluorescence images were digitized using an LSM 780 confocal microscope (Carl Zeiss, Oberkochen, Germany). Bacteria located inside HepG2 cells were counted as intercellular *P. gingivalis*, whereas those located outside of the cells or in the marginal region were not counted. At least 100 bacteria were analyzed in each experiment, with three independent experiments performed. The completely merged spots were counted manually in entire fields of view and expressed as percentages of the total internalized bacteria. The ratio of bacterial co-localization with each target marker was calculated as the percentage of total intercellular *P. gingivalis*.

### 2.6. Western blot analysis

Cells were rinsed twice with ice-cold PBS and then lysed in a buffer (50 mM Tris-HCl [pH 8.0], 1% Nonidet P-40, 0.5% sodium deoxycholate, 0.1% sodium dodecyl sulfate, 150 mM NaCl, and proteinase inhibitor cocktail). The protein concentration of each sample was measured with BCA Protein Assay Reagent (Thermo Pierce, Rockford, IL, USA). The lysate protein (5 μg) was resolved on an SDS-PAGE gel and electroblotted onto a polyvinylidene difluoride membrane. The blots were blocked with 3% milk/Tris-buffered saline with 0.1% Tween 20 for 1 h at room temperature, probed with various Abs overnight at 4 °C, washed, incubated with horseradish-peroxidase-conjugated secondary Abs (anti-rabbit IgG, 1:2000; and anti-mouse IgG, 1:2000; Cell Signaling Technology), and finally detected with ECL-Prime (GE Healthcare Life Sciences, Tokyo, Japan). The immunoreactive bands were analyzed using an LAS 4000 mini (Fujifilm, Tokyo, Japan), and Image Reader software/Multi Gauge software.

### 2.7. Cell viability assay

HepG2 cells were plated into 96-well cell culture plates containing 100 μl of cell culture medium, in triplicates, and

then treated with different concentrations of OA. After 24 h of incubation, cells were infected with *P. gingivalis*. The cells were incubated with the Cell Counting Kit-8 solution (Dojindo, Kumamoto, Japan) for 1 h and the absorbance at 450 nm was then measured with a microplate reader (iMark; Bio-Rad, Hercules, CA, USA).

### 2.8. Statistical analysis

All values are expressed as the means ± standard deviations for three independent experiments. The Tukey-Kramer method was used to identify differences between concentrations when the analysis of variance indicated a significant difference ($*P < 0.05$ or $**P < 0.01$). Alternatively, two-factor analysis of variance was used.

## 3. Results

### 3.1. *Internalized* P. gingivalis *is not localized in lipid droplets but in autophagosomes and lysosomes in HepG2 cells*

Previous studies have shown that addition of OA into the culture media in HepG2 cells can induce an experimental in vitro model of hepatic steatosis [2,21]. Therefore, we first examined the accumulation of lipid droplets in OA-induced HepG2 cells by treating the cells with 2.0 mM OA for 24 h. Untreated cells were used as the control. ORO staining revealed that OA-treated HepG2 cells had accumulated intracellular lipid droplets, whereas untreated control cells were almost devoid of intracellular lipid (Fig. 1A). After OA-induced (0–2.5 mM OA) HepG2 cells were infected with or without *P. gingivalis* for 20 min at an MOI of $10^2$, the cell viability was measured. No significant changes of cell viability were observed between the infected and uninfected cells (Fig. 1B). Under these conditions, we analyzed the subcellular localization of intracellular *P. gingivalis* (MOI of $10^2$) in the lipid-droplets-accumulated HepG2 cells. The bacteria were localized exclusively in LAMP2 (a representative lysosome marker)-positive compartments (Fig. 1C and E), and were partially co-localized with LC3, which is known to be a specific marker protein of autophagosomes (Fig. 1D and F). However, the bacteria were not detected in the ORO-stained lipid droplets during the 6–48 h post-infection period (Fig. 1C and D).

### 3.2. *Lipid droplets increase the existence of* P. gingivalis *in HepG2 cells at an early phase of infection*

Next, we investigated the effects of lipid droplets on internalization and persistence of *P. gingivalis* in HepG2 cells. OA-treated and untreated HepG2 cells were respectively pre-incubated with viable *P. gingivalis* for 20 min, and then further incubated for various times without the bacteria. After lysis of the cells, the numbers of anaerobic colonies on agar plates were determined. The numbers of internalized bacteria between OA-treated and untreated HepG2 cells were comparable (Fig. 1G). However, OA-induced HepG2 cells exhibited significantly higher bacterial numbers at 6 h after infection than did untreated cells, although both cell types showed similar bacterial numbers during the 12–48 h post-infection period (Fig. 1H). These results indicate that the presence of lipid droplets increases the bacterial existence in HepG2 cells at an early phase of infection.

### 3.3. *Lipid droplets affect formation of autolysosomes for elimination of* P. gingivalis

To further investigate how lipid droplets affect the elimination of *P. gingivalis* in hepatocytes, we compared the intracellular trafficking of *P. gingivalis* in OA-treated and untreated HepG2 cells during 6–48 h of incubation. Confocal microscopic analysis of normal OA-untreated HepG2 cells revealed the DAPI-stained *P. gingivalis* to be mainly in LAMP2-positive compartments (lysosomes) throughout the 6–48 h post-infection period (Fig. 2A). The internalized *P. gingivalis* cells were partially co-localized with LC3 (Fig. 2A). The LAMP2-positive and LC3-positive ($LAMP2^+$/$LC3^+$) puncta gradually increased with time in these control cells (Fig. 2A). In the OA-treated HepG2 cells, the internalized *P. gingivalis* cells were also found mainly in LAMP2-positive compartments and were partially co-localized in LC3-positive vesicles (Fig. 2B). However, the formation of LC3 puncta was apparently decreased compared with that in untreated control HepG2 cells (Fig. 2B).

### 3.4. *Time course of formation of autolysosomes for elimination of* P. gingivalis

Based on quantitative analysis of the confocal microscopic observations (Fig. 2A and B), we classified into three-types compartments, i.e. $LC3^+$/$LAMP2^-$ compartments (autophagosomes), $LC3^+$/$LAMP2^+$ compartments (autolysosomes), and $LC3^-$/$LAMP2^+$ compartments (late endosomes/lysosomes). The percentages of co-localization of intracellular *P. gingivalis* with $LC3^+$/$LAMP2^+$ compartments in the untreated HepG2 cells were significantly higher than those in OA-treated HepG2 cells throughout the 12–48 h post-infection period (Fig. 3B). By contrast, the percentages of co-localization of *P. gingivalis* with $LC3^-$/$LAMP2^+$ compartments in OA-treated HepG2 cells were significantly higher than in control HepG2 cells during the 12–48 h post-infection period (Fig. 3B). Since LC3 exists in an 18 kDa cytosolic form (LC3-I) and a processed 16 kDa form (LC3-II) on the autophagosomal membrane, we examined for LC3-II formation in HepG2 cells infected with *P. gingivalis* (Fig. 3C). To test the effects of lipid droplets on autophagy flux, we utilized bafilomycin $A_1$ (Baf), a specific inhibitor of V-ATPase, which inhibits fusion between autophagosomes and lysosomes [10,11]. Upon Baf treatment for *P. gingivalis*-infected HepG2 cells under OA-uninduced conditions, the protein levels of LC3II in Baf-treated cells were significantly higher than those of Baf-untreated

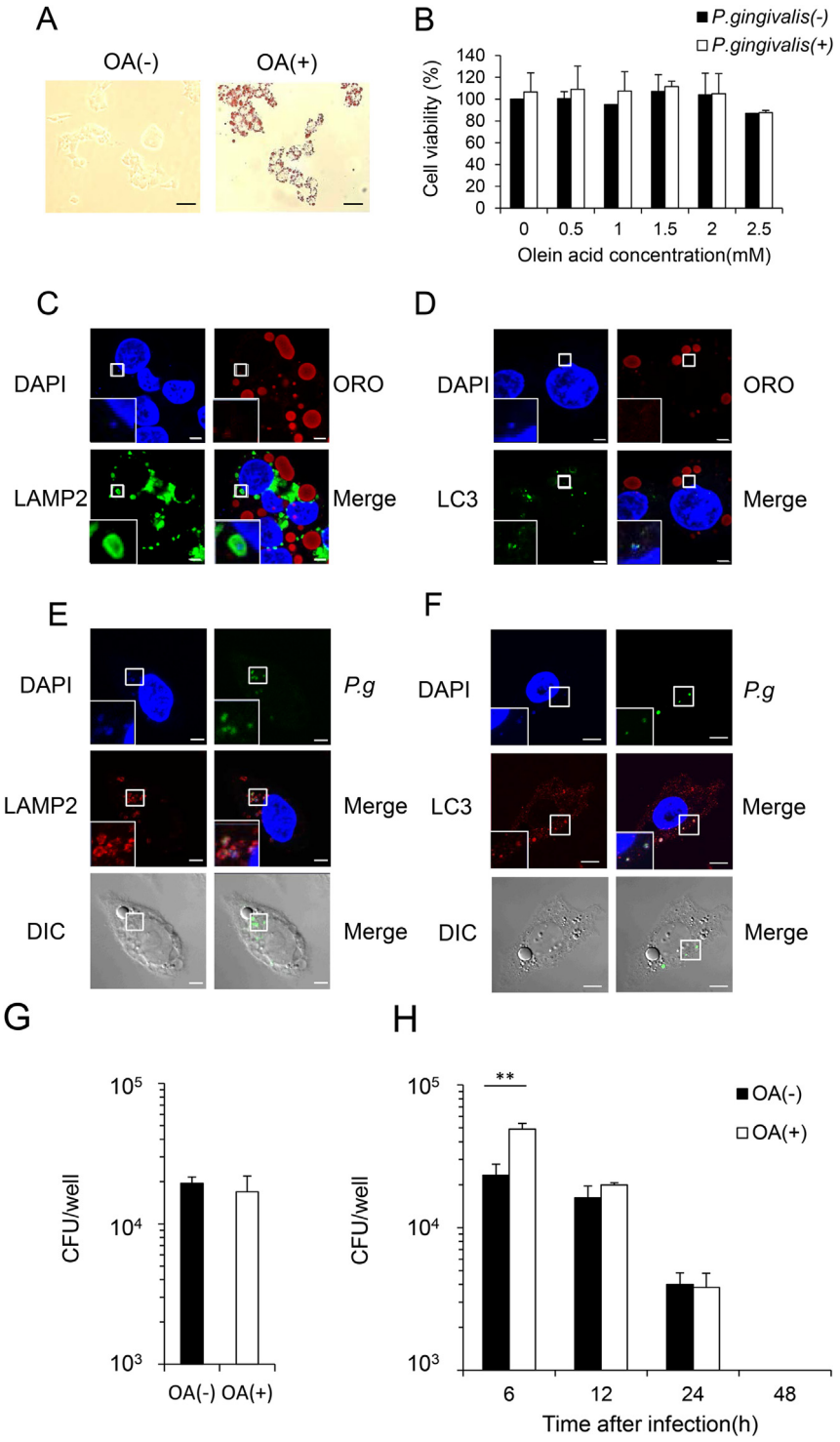


Fig. 1. Effects of *Porphyromonas gingivalis* infection on the cell viability of oleic-acid (OA)-induced HepG2 cells, and study of its localization in the lipid-droplets-accumulated cells. (A) Formation of lipid droplets in control or OA-induced HepG2 cells. Bar = 50 μm. (B) HepG2 cells were treated with 0–2.5 mM OA for 24 h. After infection with *P. gingivalis* at an MOI of $10^2$ for 20 min, cell viability was analyzed using a commercial cell counting kit. Results are representative of three independent experiments. (C–F) Confocal microscopic images of intracellular *P. gingivalis* in lipid droplets-induced HepG2 cells. After infection with *P. gingivalis* at an MOI of $10^2$ for 20 min, OA-induced HepG2 cells were washed and further cultured for 24 h in the absence of extracellular bacteria and then stained with DAPI, oil red O (ORO), or antibodies against lysosome-associated membrane protein 2 (LAMP2) or microtubule-associated protein 1 light chain 3 (LC3). (C, D) Localization of the bacterial cell type (blue), ORO (red), and LAMP2 or LC3 (green) was analyzed by confocal microscopy. Bar = 5 μm. (E, F) Localization of intracellular *P. gingivalis* (green), LAMP2 or LC3 (red), the nuclei (blue), and DIC images were analyzed by confocal microscopy. Bar = 5 μm. (G, H) Internalization and existence of infected *P. gingivalis* in control or lipid droplets-induced HepG2 cells. HepG2 cells ($1 \times 10^5$ cells per well) were infected with *P. gingivalis* for 20 min at an MOI of $10^2$. After infection, the further incubated cells were lysed at the indicated times, and the lysates were 10-fold serially diluted and plated onto CDC anaerobe blood agar plates. Data are the means ± standard deviation of values from three independent experiments ($P < 0.05$, compared with the values for control cells). (G) Internalization efficiency of the bacteria (0 h), (H) The bacterial existence after the infection period (6–48 h).

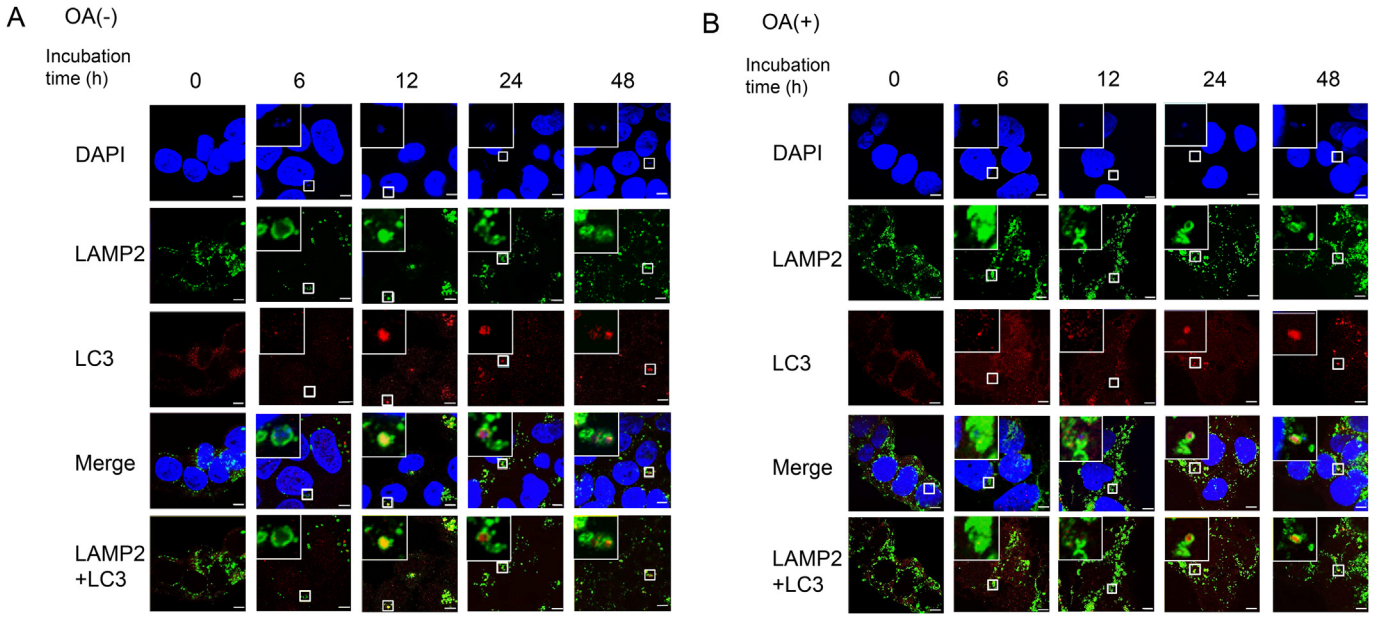


Fig. 2. Confocal microscopic images of intracellular *Porphyromonas gingivalis*-infected HepG2 cells. (A) Control HepG2 cells. (B) Oleic acid (OA)-induced HepG2 cells. After infection with *P. gingivalis* (MOI = $10^2$) for 20 min, the cells were washed and further cultured for the indicated times (0–48 h) in the absence of extracellular bacteria and then stained with DAPI (blue) or antibodies against lysosome-associated membrane protein 2 (LAMP2) (green) or microtubule-associated protein 1 light chain 3 (LC3) (red). Localization of the bacterial cells, LAMP2, and LC3 was analyzed by confocal microscopy. The data are representative of at least three independent experiments. Bar = 5 μm.

cells during 0–6 h of incubation (Fig. 3C and D). Under OA-induced conditions, however, the protein levels of LC3II between Baf-treated and untreated cells were statistically comparable at 6 h of incubation (Fig. 3C and D). These results indicate that autophagy flux was partially inhibited under OA-induced conditions at an early phase of infection. Thus, an accumulation of lipid droplets affects the formation of lysosomes and autolysosomes for elimination of *P. gingivalis*, implying the delayed elimination of the bacteria in hepatic steatosis-induced HepG2 cells at an early phase of infection.

## 4. Discussion

In this study, we demonstrated that OA-induced lipid droplets in HepG2 cells increase the persistence of *P. gingivalis* at an early phase of infection. The presence of intracellular lipid droplets affects the formation of autolysosomes for the elimination of the bacterial cells. Thus, lipid droplets are likely to affect the persistence of *P. gingivalis* in HepG2 cells by altering the autophagy-lysosome systems.

Distinct from some bacteria and parasites that usurp lipid droplets [14,18], it is unlikely that *P. gingivalis* uses lipid droplets as a nutrient source or as assembly platforms during their infection. This notion is based on the findings that *P. gingivalis* was not localized in the lipid droplets and that prolonged persistence of the bacteria was not observed in hepatic steatosis-induced HepG2 cells. However, the present study showed that the presence of lipid droplets increased the persistence of *P. gingivalis* in HepG2 cells at an early phase of infection. In addition to the decreased elimination of the bacteria within hepatocytes, a previous study showed that accumulation of lipid droplets led to up-regulation of Toll-like receptor 2 and thereby enhanced the production of pro-inflammatory cytokines [6]. Considering these synergic effects, it is reasonable to speculate that an accumulation of lipid droplets causes excessive inflammatory responses and thereby inflammatory exacerbation in hepatocytes.

The presence of intracellular lipid droplets affected the formation of lysosomes and the process of autophagy for eliminating *P. gingivalis*. In particular, the differences in time-course co-localization of *P. gingivalis* with autolysosomes and lysosomes may be directly associated with the increased persistence of the bacteria in HepG2 cells at an early phase of infection. Recently, crosstalk between lipid droplets and lysosomes through autophagy has been suggested [5]. The lysosome-mediated lipid droplet degradation system, termed “lipophagy”, was first discovered in studies of lipid accumulation in liver-specific autophagy-related gene 5 (Atg5) or 7 (Atg7) knockout mice [17]. Considering the accumulation of lipid droplets as degradation organelles by the autophagy–lysosome system [5], it is likely that intracellular lipid droplets can affect the formation of lysosomes and the autophagy system for elimination of intracellular bacteria, which is known as “xenophagy” [13,8]. It would be interesting to determine the detailed molecular mechanisms of lipophagy and xenophagy against *P. gingivalis* infection in lipid-loaded cells other than hepatocytes.

In conclusion, the delayed elimination of *P. gingivalis* by intracellular lipid accumulation may cause prolonged

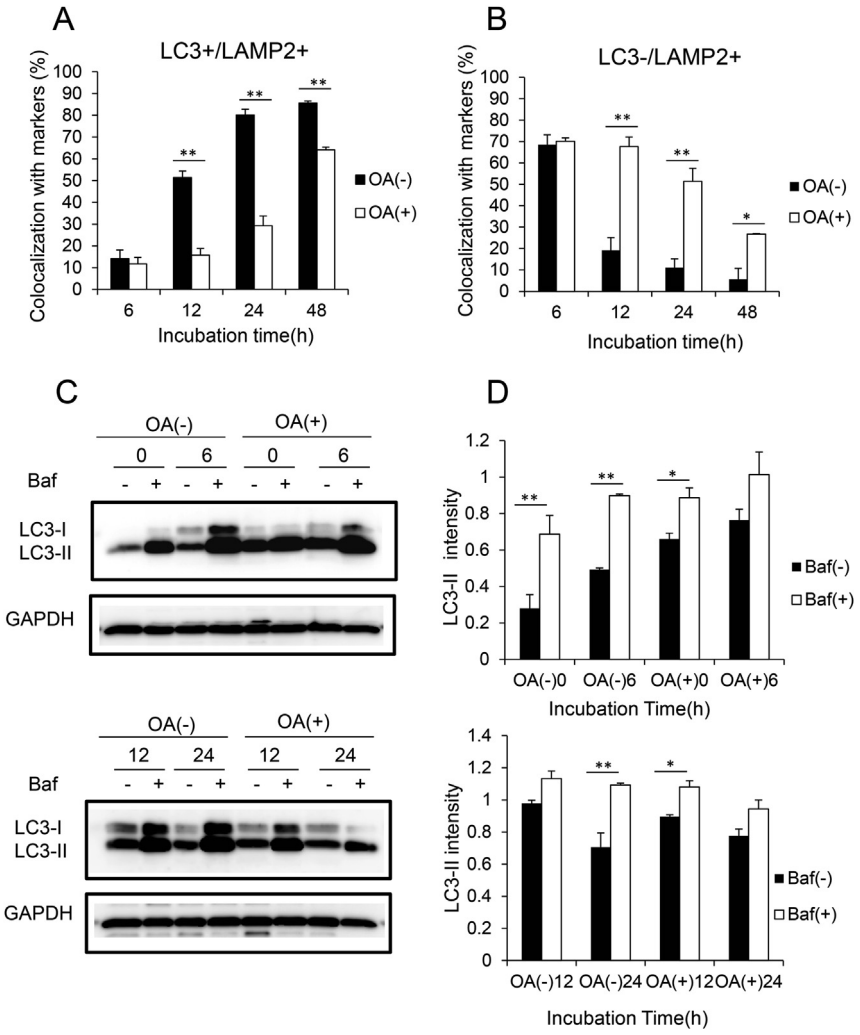


Fig. 3. Time-course analysis of the co-localization of *Porphyromonas gingivalis* with microtubule-associated protein 1 light chain 3 (LC3) and lysosome-associated membrane protein 2 (LAMP2) compartments, and LC-II formation by western blotting. (A, B) The percentages of co-localization of *P. gingivalis* with LAMP2 or LC3 were quantified from images obtained by confocal microscopy at each time point. Data are the means and standard deviation from three independent experiments. (A) $LC3^{+}/LAMP2^{+}$ compartments. (B) $LC3^{-}/LAMP2^{+}$ compartments. (C) Western blot analysis of the processed form of LC3 (LC3-II) in HepG2 cells infected with *P. gingivalis* in the presence or absence of bafilomycin $A_1$ (Baf). Cells were preincubated for 90 min with or without $5 \times 10^{-7}$ M Baf. After *P. gingivalis* infection, oleic-acid (OA)-induced or uninduced-HepG2 cells were further incubated for the indicated time. The cell lysates of the respective infected cells were subjected to SDS-PAGE and western blot analysis with the anti-LC3 antibody or anti-LAMP2 antibody. The data are representative of three independent experiments. (D) A densitometric analysis for the quantification of processed and cytosolic forms of LC3 (LC3-II/LC3-I) in the cell lysate at the indicated incubation times. The density was measured with an LAS 4000 mini image analyzer, and the arbitrary density unit was defined as the relative intensity of LC3-II/GAPDH obtained with the same samples. The data are the means ± standard deviation from three independent experiments. $*P < 0.05$, $**P < 0.01$, compared with the value between Baf-treated and untreated cells.

inflammation and cellular damage, and is one of the risk factors for the development and progression of NAFLD.

## Conflict of interest

The authors declare no conflicts of interest.

## Acknowledgments

We thank Drs. Koji Nakayama, Kuniaki Okamoto, Kazuhisa Nishishita, Eiko Sakai and Mikio Shoji for useful comments. This work was supported by JSPS KAKENHI grant numbers 25293383, 15H05298, 26670906, 25462892, 30264055, and 16K15790.

## References

[1] Bostanci N, Belibasakis GN. *Porphyromonas gingivalis*: an invasive and evasive opportunistic oral pathogen. FEMS Microbiol Lett 2012;333:1–9.

[2] Cui W, Chen SL, Hu KQ. Quantification and mechanisms of oleic acid-induced steatosis in HepG2 cells. Am J Transl Res 2010;2:95–104.

[3] Deshpande RG, Khan MB, Genco CA. Invasion of aortic and heart endothelial cells by *Porphyromonas gingivalis*. Infect Immun 1998;66:5337–43.

[4] Dorn BR, Dunn WA, Progulske-Fox A. *Porphyromonas gingivalis* traffics to autophagosomes in human coronary artery endothelial cells. Infect Immun 2001;69:5698–708.

[5] Dugail I. Lysosome/lipid droplet interplay in metabolic diseases. Biochimie 2014;96:102–5.

[6] Furusho H, Miyauchi M, Hyogo H, Inubushi T, Ao M, Ouhara K, et al. Dental infection of *Porphyromonas gingivalis* exacerbates high fat diet-induced steatohepatitis in mice. J Gastroenterol 2013;48:1259–70.
[7] Kadowaki T, Takii R, Yamatake K, Kawakubo T, Tsukuba T, Yamamoto K. A role for gingipains in cellular responses and bacterial survival in *Porphyromonas gingivalis*-infected cells. Front biosci J Virtual Libr 2007;12:4800–9.
[8] Knodler LA, Celli J. Eating the strangers within: host control of intracellular bacteria via xenophagy. Cell Microbiol 2011;13:1319–27.
[9] Lamont RJ, Oda D, Persson RE, Persson GR. Interaction of *Porphyromonas gingivalis* with gingival epithelial cells maintained in culture. Oral Microbiol Immunol 1992;7:364–7.
[10] Mauvezin C, Nagy P, Juhasz G, Neufeld TP. Autophagosome-lysosome fusion is independent of V-ATPase-mediated acidification. Nat Commun 2015;6:7007.
[11] Mizushima N, Yoshimori T. How to interpret LC3 immunoblotting. Autophagy 2007;3:542–5.
[12] Nakayama K, Kadowaki T, Okamoto K, Yamamoto K. Construction and characterization of arginine-specific cysteine proteinase (Arg-gingipain)-deficient mutants of *Porphyromonas gingivalis*. Evidence for significant contribution of Arg-gingipain to virulence. J Biol Chem 1995;270:23619–26.
[13] Noda T, Yoshimori T. Molecular basis of canonical and bactericidal autophagy. Int Immunol 2009;21:1199–204.
[14] Saka HA, Valdivia R. Emerging roles for lipid droplets in immunity and host-pathogen interactions. Annu Rev Cell Dev Biol 2012;28:411–37.
[15] Sandros J, Papapanou P, Dahlen G. *Porphyromonas gingivalis* invades oral epithelial cells in vitro. J Periodontal Res 1993;28:219–26.
[16] Sandros J, Papapanou PN, Nannmark U, Dahlen G. *Porphyromonas gingivalis* invades human pocket epithelium in vitro. J Periodontal Res 1994;29:62–9.
[17] Singh R, Kaushik S, Wang Y, Xiang Y, Novak I, Komatsu M, et al. Autophagy regulates lipid metabolism. Nature 2009;458:1131–5.
[18] Stehr M, Elamin AA, Singh M. Cytosolic lipid inclusions formed during infection by viral and bacterial pathogens. Microbes Infection Institut Pasteur 2012;14:1227–37.
[19] Takeuchi H, Furuta N, Amano A. Cell entry and exit by periodontal pathogen via recycling pathway. Commun Integr Biol 2011;4:587–9.
[20] Takeuchi H, Furuta N, Morisaki I, Amano A. Exit of intracellular *Porphyromonas gingivalis* from gingival epithelial cells is mediated by endocytic recycling pathway. Cell Microbiol 2011;13:677–91.
[21] Vidyashankar S, Sandeep Varma R, Patki PS. Quercetin ameliorate insulin resistance and up-regulates cellular antioxidants during oleic acid induced hepatic steatosis in HepG2 cells. Toxicol Vitro 2013;27:945–53.
[22] Yamatake K, Maeda M, Kadowaki T, Takii R, Tsukuba T, Ueno T, et al. Role for gingipains in *Porphyromonas gingivalis* traffic to phagolysosomes and survival in human aortic endothelial cells. Infect Immun 2007;75:2090–100.
[23] Yoneda M, Naka S, Nakano K, Wada K, Endo H, Mawatari H, et al. Involvement of a periodontal pathogen, *Porphyromonas gingivalis* on the pathogenesis of non-alcoholic fatty liver disease. BMC Gastroenterol 2012;12:16.